

See discussions, stats, and author profiles for this publication at: <https://www.researchgate.net/publication/222090255>

# DFT and Ab Initio Study on Mechanism of Olefin Hydroalumination by $\text{XAlBu}_2$ in the Presence of $\text{Cp}_2\text{ZrCl}_2$ Catalyst. II. Olefin Interaction with Catalytically Active Centers

ARTICLE in ORGANOMETALLICS · JULY 2013

Impact Factor: 4.13 · DOI: 10.1021/om200518h

CITATIONS

11

READS

47

6 AUTHORS, INCLUDING:



Evgeniy Yu. Pankratyev

Russian Academy of Sciences

11 PUBLICATIONS 68 CITATIONS

SEE PROFILE



Lyudmila V. Parfenova

Russian Academy of Sciences

26 PUBLICATIONS 127 CITATIONS

SEE PROFILE



Sergey Khursan

Russian Academy of Sciences

162 PUBLICATIONS 544 CITATIONS

SEE PROFILE



Leonard Khalilov

Russian Academy of Sciences

327 PUBLICATIONS 997 CITATIONS

SEE PROFILE

# DFT and Ab Initio Study on Mechanism of Olefin Hydroalumination by $\text{XAlBu}_2$ in the Presence of $\text{Cp}_2\text{ZrCl}_2$ Catalyst. II. <sup>1</sup> Olefin Interaction with Catalytically Active Centers

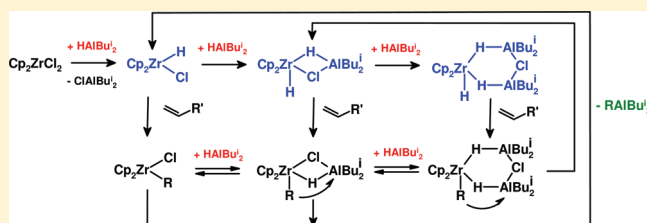
Evgeniy Yu. Pankratyev,<sup>†</sup> Tatyana V. Tyumkina,<sup>†</sup> Lyudmila V. Parfenova,<sup>†</sup> Sergey L. Khursan,<sup>‡</sup> Leonard M. Khalilov,<sup>\*,†</sup> and Usein M. Dzhemilev<sup>†</sup>

<sup>†</sup>Institute of Petrochemistry and Catalysis, Russian Academy of Sciences, Prospekt Oktyabrya, 141, 450075 Ufa, Russia

<sup>‡</sup>Institute of Organic Chemistry, Ufa Scientific Center, Russian Academy of Sciences, Prospekt Oktyabrya, 71, 450054 Ufa, Russia

## Supporting Information

**ABSTRACT:** The mechanism of alkene hydroalumination by  $\text{HAlBu}_2$  catalyzed with  $\text{Cp}_2\text{ZrCl}_2$  has been studied computationally at the DFT and MP2 levels of theory. The mechanism involves several catalytic cycles with the following stages: active center formation, alkene hydrozirconation, transmetalation, and regeneration of key intermediates. The complexes  $\text{Cp}_2\text{ZrHCl}$ ,  $[\text{Cp}_2\text{ZrH}_2 \cdot \text{ClAlBu}_2]$ ,  $[\text{Cp}_2\text{ZrH}_2 \cdot \text{HAlBu}_2 \cdot \text{ClAlBu}_2]$ , and  $[\text{Cp}_2\text{ZrH}_2 \cdot (\text{HAlBu}_2)_2]$  are considered as active species of the catalytic process. It has been shown that the hydrometalation ability of the complexes decreases in the series  $\text{Cp}_2\text{ZrHCl} > [\text{Cp}_2\text{ZrH}_2 \cdot \text{ClAlBu}_2] > [\text{Cp}_2\text{ZrH}_2 \cdot \text{HAlBu}_2 \cdot \text{ClAlBu}_2] > [\text{Cp}_2\text{ZrH}_2 \cdot (\text{HAlBu}_2)_2]$ ; this is caused by an increase in the number of  $\text{Zr}-\text{H}-\text{Al}$  bridge bonds as a result of consecutive  $\text{HAlBu}_2$  addition. For comparison, thermodynamic and activation parameters of a noncatalytic propene reaction with  $\text{HAlBu}_2$  were calculated.



## INTRODUCTION

The reactions of direct thermal alkene hydroalumination with organoaluminum compounds (OACs) containing  $\text{Al}-\text{H}$  bonds occur at temperatures above 340 K.<sup>2</sup> However, the use of transition metal complex catalysts allows significant reduction of the reaction temperature and pressure, and it radically improves stereoselectivity. It is proposed that the active intermediates of the catalytic alkene hydroalumination are metal hydrides, which are formed in the catalytic cycle.<sup>3,4</sup> These assumptions were based on results of Schwarz's investigations on alkene hydrozirconation by  $\text{Cp}_2\text{ZrHCl}$ .<sup>5</sup> Recently we carried out experimental studies on the mechanism of the olefin hydroalumination by alkylalanes ( $\text{HAlBu}_2$ ,  $\text{ClAlBu}_2$ , and  $\text{AlBu}_3$ ), catalyzed with  $\text{Cp}_2\text{ZrCl}_2$ ,<sup>6</sup> and we proposed the dimeric  $\text{Zr},\text{Al}$ -hydride complex  $[\text{Cp}_2\text{ZrH}_2 \cdot \text{ClAlBu}_2]_2$  (7) as being the key intermediate. Zirconocene hydrochloride,  $\text{Cp}_2\text{ZrHCl}$ , was assumed to be one of the reaction intermediates, which appears in situ, immediately reacts with the initial OAC, and gives the dimeric complex 7. Its interaction with  $\text{HAlBu}_2$  yields the complex  $[\text{Cp}_2\text{ZrH}_2 \cdot \text{ClAlBu}_2 \cdot \text{HAlBu}_2]$  (8), which was considered as inactive in the olefin hydrometalation. These experimental results initiated computational investigation of the mechanism of intermediate formation in the  $\text{Cp}_2\text{ZrCl}_2-\text{HAlBu}_2$  system using density functional theory (DFT).<sup>1</sup> The results of this theoretical study are presented in Scheme 1.

The DFT calculations confirmed the possibility that both  $\text{Cp}_2\text{ZrHCl}$  and dimeric complex 7 form in the reaction.

Moreover, the set of  $\text{Zr},\text{Al}$  complexes that could exist in the system  $\text{Cp}_2\text{ZrCl}_2-\text{HAlBu}_2$  has been considerably extended. Simultaneously with this work, complexes 9 and 12 were experimentally found elsewhere by NMR.<sup>7</sup> Thus,  $\text{Cp}_2\text{ZrHCl}$  as well as all proposed  $\text{Zr},\text{Al}$ -hydrides should be considered as possible key intermediates of the hydrometalation.

The reaction of ethylene hydrozirconation by  $\text{Cp}_2\text{ZrHCl}$  was studied earlier by the means of quantum chemical calculations using RHF and MP2(fc) methods.<sup>8</sup> However, to the best of our knowledge, there have been no theoretical studies on olefin hydrometalation with bimetallic  $\text{Zr},\text{Al}$ -hydride complexes. Therefore, in this work we report a detailed DFT study of the alkene reaction with intermediates formed in the hydroalumination reaction; we believe that this study is essential for determining the key catalytic complexes in this process.

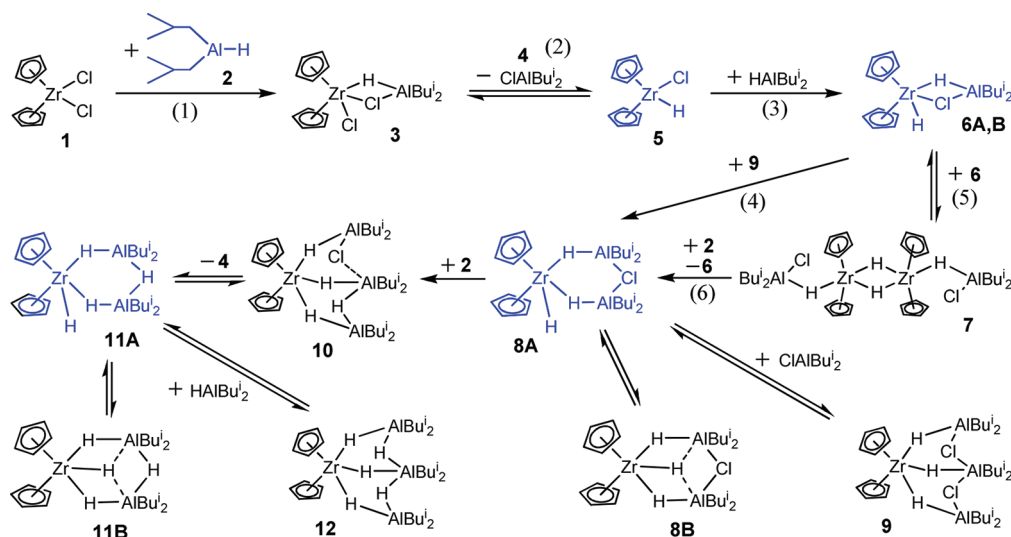
## COMPUTATIONAL DETAILS

Geometry optimization for the compounds, vibrational frequency analysis, transition state (TS) searches of the studied transformations and intrinsic reaction coordinate calculations (IRC) were carried out using the PRIRODA 06 program<sup>9</sup> with the Perdew–Burke–Ernzerhof<sup>10</sup> (PBE) functional in combination with a 3 $\zeta$  basis set.<sup>9c</sup> The IRC pathways were calculated for each TS obtained in order to verify the nature of this TS. Thermodynamic parameters and activation energies were determined

Received: June 16, 2011

Published: November 03, 2011

Scheme 1



at 203 K, because complexes 7 and 8 were observed simultaneously in the NMR spectra at this temperature.<sup>6a</sup>

Using the equilibrium geometry parameters, entropy, and thermodynamic corrections, obtained by means of PBE/3 $\zeta$ , the total energy and thermodynamic functions of compounds were calculated in the RI-MP2/ $\Lambda$ 2 approach,<sup>11,12</sup> which takes into account relativistic effects.

Nonpolar solvent (toluene) effects on the energy parameters of the compounds and reactions has been accounted for. Solvation correction to the energy characteristics was calculated as the difference between the total energy in solution and gas phase. Full energies, included in the solvation correction expression, were calculated using the equilibrium geometrical parameters obtained by the PBE/3 $\zeta$  method, using the ORCA 2.6 Rev. 35<sup>13</sup> program in the RI-PBE/TZVP approach.<sup>10,14</sup> The total energy of molecules in solution was calculated with the polarized continuum COSMO method.<sup>15</sup>

Visualization of quantum chemical data was carried out with the programs QCC Front-End<sup>16</sup> and ChemCraft.<sup>17</sup>

## RESULTS AND DISCUSSION

**Choice of Calculation Model and Level of Theory.** The PBE/3 $\zeta$  approximation used provides a correct reproduction of geometry parameters of the studied compounds.<sup>18</sup> Thus, we have shown earlier a good agreement between calculated and experimental structures of organoaluminum (the geometry for the AlMe<sub>3</sub> dimer was taken from X-ray data,<sup>18a</sup> while that for the AlMe<sub>3</sub> monomeric form was obtained by gas-phase electron diffraction<sup>18b</sup>) and organozirconium compounds (X-ray experiment for Cp<sub>2</sub>ZrCl<sub>2</sub><sup>1</sup>).

It is known that DFT methods underestimate the bridge bond energy, such as Al–X–Al (X = C, H, Cl).<sup>18</sup> In this regard, we have studied the effect of various DFT functionals (PBE, mPBE, PBE1, BLYP, B3LYP, OLYP, and B3LYP\_PW) and basis sets (3 $\zeta$ , two-exponential  $\Lambda$ 1, three-exponential  $\Lambda$ 2, and four-exponential  $\Lambda$ 3)<sup>18b</sup> on the trimethylaluminum dimerization energy, taken as a test system. It was shown that the PBE functional provides the most adequate results, and an enhancement of the basis set does not lead to a significant change in the energy of the AlMe<sub>3</sub> dimer. It was also revealed that the RI-MP2/ $\Lambda$ 2//PBE/3 $\zeta$  level of theory quantitatively reproduces the testing energy. Therefore, the latter method was chosen as the basic approximation to study of reaction

energetics with participation of bridged complexes. It is noteworthy that, depending on the nature of X, the PBE/3 $\zeta$  method underestimates the Al–X–Al bridge energy in the dimerization reaction by 3.0 kcal/mol per bond for AlMe<sub>3</sub>, 5.4 kcal/mol for AlEt<sub>3</sub>,<sup>18a</sup> and 6.8 kcal/mol for AlBu<sub>3</sub>,<sup>18c</sup> whereas this underestimation is only by 1.6 kcal/mol for HAlBu<sub>2</sub> (X = H) and 3.4 kcal/mol for ClAlBu<sub>2</sub> (X = Cl)<sup>18d</sup> in comparison to the baseline method. This comparison indicates that the stronger the bridge bond, the more adequate is the DFT method.

To obtain more reliable reaction energetics in solution, the nonspecific solvation effects of toluene on the reaction Gibbs energy were taken into account. Solvation calculations were performed using the COSMO model of solvent in the RI-PBE/TZVP approximation. Thus, the thermodynamic characteristics of reactions 1–6 (Scheme 1), previously studied by means of the PBE/3 $\zeta$  method,<sup>1</sup> were improved at the MP2 level of theory on taking solvation into account. Nevertheless, we should note that in most cases of our model calculations the PBE/3 $\zeta$  approximation describes correctly the trends determined at the RI-MP2/ $\Lambda$ 2//PBE/3 $\zeta$  level of theory (Table 1).

To simplify the quantum chemical description, we used the monomeric form of HAlBu<sub>2</sub> in the modeling of the alkene hydroalumination reactions. It is possible that the reactions of the HAlBu<sub>2</sub> monomer can occur under the conditions of its formation in situ: for example, in the systems Cp<sub>2</sub>ZrCl<sub>2</sub>–ClAlBu<sub>2</sub> and Cp<sub>2</sub>ZrCl<sub>2</sub>–AlBu<sub>3</sub>. However, in these cases the possibility of complexation of various OAC types providing mixed associates cannot be disregarded. When HAlBu<sub>2</sub> is used as the initial organoaluminum reagent, it is necessary to consider the contribution of its dimeric and trimeric forms. Thus, recently<sup>18d</sup> we have carried out a simulation of the associative processes occurring in HAlBu<sub>2</sub> and ClAlBu<sub>2</sub> systems (up to the formation of OAC tetrameric forms) in the RI-MP2/ $\Lambda$ 2//PBE/3 $\zeta$  approach, taking into account nonspecific solvation by toluene, calculated by means of the COSMO method in the PBE/6-311+G(d,p) approach. It was shown that the equilibrium concentration of the monomeric form lies in the interval of 10<sup>–14</sup>–10<sup>–9</sup> mol/L, depending on the reaction temperature (203–298 K); this estimation was done for the overall concentration of HAlBu<sub>2</sub> of 1.0 mol/L. The competing reactions between Cp<sub>2</sub>ZrCl<sub>2</sub> and monomeric,

**Table 1.** Calculated Thermodynamic Parameters for Reactions 1–26 at  $T = 203\text{ K}$  ( $\Delta S$  (cal/(mol K));  $\Delta H$ ,  $\Delta G$  (kcal/mol)) at the PBE/3 $\zeta$  (RI-MP2/ $\Lambda$ 2//PBE/3 $\zeta$  in Parentheses) Level of Theory

reacn	$\Delta S^\circ$	$\Delta H^\circ$	$\Delta G^\circ$	$\Delta G^\circ_{\text{solv}}$	$\Delta S^\ddagger$	$\Delta H^\ddagger$	$\Delta G^\ddagger$	$\Delta G^\ddagger_{\text{solv}}$
1	−42.7 <sup>1</sup>	−18.8 <sup>1</sup> (−28.8)	−10.2 <sup>1</sup> (−20.2)	−2.4 (−12.4)				
2	44.7 <sup>1</sup>	15.1 <sup>1</sup> (27.3)	6.0 <sup>1</sup> (18.3)	4.3 (16.6)				
3 → LM	7.1 <sup>1</sup>	1.9 <sup>1</sup> (4.8)	0.4 <sup>1</sup> (3.4)	−0.2 (2.8)	−0.8 <sup>1</sup>	2.8 <sup>1</sup> (5.8)	2.9 <sup>1</sup> (6.0)	2.6 (5.7)
LM → 5 + 4	37.6 <sup>1</sup>	13.2 <sup>1</sup> (22.5)	5.6 <sup>1</sup> (14.9)	4.4 (13.7)				
3	−42.6 <sup>1</sup>	−25.4 <sup>1</sup> (−35.0)	−16.8 <sup>1</sup> (−26.3)	−8.5 (−18.0)				
4	−40.0 <sup>1</sup>	−19.3 <sup>1</sup> (−28.6)	−11.2 <sup>1</sup> (−20.5)	−3.2 (−12.5)				
6A + 2 → LM	−33.4 <sup>1</sup>	−5.0 <sup>1</sup> (−12.2)	1.8 <sup>1</sup> (−5.4)	9.2 (2.0)				
LM → 8A	−6.6 <sup>1</sup>	−14.3 <sup>1</sup> (−16.4)	−13.0 <sup>1</sup> (−15.1)	−12.4 (−14.5)	−7.4 <sup>1</sup>	4.7 <sup>1</sup> (6.8)	6.2 <sup>1</sup> (8.3)	6.3 (8.4)
5	−45.9 <sup>1</sup>	−6.6 <sup>1</sup> (−25.0)	2.7 <sup>1</sup> (−15.7)	3.0 (−15.4)				
6A + 6A → LM	−46.8 <sup>1</sup>	3.4 <sup>1</sup> (−13.4)	12.9 <sup>1</sup> (−3.9)	14.0 (−2.8)	−38.8 <sup>1</sup>	9.6 <sup>1</sup> (3.0)	17.5 <sup>1</sup> (10.8)	18.9 (12.2)
LM → 7	1.0 <sup>1</sup>	−10.0 <sup>1</sup> (−11.6)	−10.2 <sup>1</sup> (−11.8)	−10.9 (−12.5)	−4.4 <sup>1</sup>	5.1 <sup>1</sup> (6.5)	6.0 <sup>1</sup> (7.3)	5.9 (7.2)
6	5.9 <sup>1</sup>	−12.7 <sup>1</sup> (−3.6)	−13.9 <sup>1</sup> (−4.8)	−6.2 (2.9)				
7 + 2 → LM <sup>a</sup>	−37.4 <sup>1</sup>	−8.4 <sup>1</sup> (−12.9)	−0.8 <sup>1</sup> (−5.3)	7.1 (2.6)				
LM → LM <sup>a</sup>	−8.6 <sup>1</sup>	6.3 <sup>1</sup> (6.3)	8.0 <sup>1</sup> (8.1)	8.3 (8.4)	−15.5 <sup>1</sup>	8.8 <sup>1</sup> (7.5)	11.9 <sup>1</sup> (10.7)	12.4 (11.2)
LM → 8A + 6A <sup>a</sup>	51.8 <sup>1</sup>	−10.6 <sup>1</sup> (4.3)	−21.1 <sup>1</sup> (−6.3)	−21.6 (−6.8)	12.7 <sup>1</sup>	1.8 <sup>1</sup> (10.6)	−0.8 <sup>1b</sup> (8.0)	−0.7 <sup>b</sup> (8.1)
7	−36.0	−24.7 (−28.0)	−17.4 (−20.7)	−10.7 (−14.0)				
13 + 2 → 15A	−33.4	−7.0 (−9.3)	−0.2 (−2.5)	6.6 (4.3)				
15A → 14A	−2.6	−17.7 (−18.7)	−17.2 (−18.2)	−17.3 (−18.3)	−7.3	6.2 (11.8)	7.6 (13.3)	8.2 (13.9)
8	−36.1	−21.7 (−25.6)	−14.4 (−18.2)	−6.8 (−10.6)				
13 + 2 → 15B	−35.3	−6.1 (−9.0)	1.1 (−1.8)	7.7 (4.8)				
15B → 14B	−0.9	−15.6 (−16.6)	−15.4 (−16.4)	−14.4 (−15.4)	−5.4	9.3 (15.7)	10.4 (16.8)	11.2 (17.6)
9	−41.3	−17.0 (−25.0)	−8.6 (−16.6)	−7.5 (−15.5)	−42.5	7.9 (1.6)	16.6 (10.3)	16.7 (10.4)
10	−37.5	−16.9 (−24.9)	−9.3 (−17.3)	−8.1 (−16.1)	−44.9	19.1 (14.6)	28.2 (23.7)	27.9 (23.4)
11	−43.6	−14.2 (−23.8)	−5.3 (−14.9)	−4.0 (−13.6)	−44.7	8.2 (1.2)	17.3 (10.3)	17.6 (10.6)
12	−44.8	−11.5 (−21.2)	−2.4 (−12.1)	−1.1 (−10.8)	−45.2	21.6 (18.0)	30.8 (27.1)	30.5 (26.8)
13	−44.2	−21.0 (−31.7)	−12.0 (−22.7)	−3.6 (−14.3)				
14	−42.9	−17.7 (−28.1)	−9.0 (−19.4)	−0.5 (−10.9)				
15	7.9	−0.4 (4.2)	−2.0 (2.6)	−3.1 (1.5)	1.8	22.5 (24.1)	22.1 (24.0)	21.1 (23.0)
16	40.3	10.4 (20.9)	2.2 (12.7)	0.4 (10.9)				
17	−35.0	−18.1 (−23.9)	−11.0 (−16.8)	−3.6 (−9.4)	−41.7	4.3 (−2.3 <sup>c</sup> )	12.8 (6.2)	20.0 (13.4)
18	−42.9	−12.6 (−21.7)	−3.8 (−13.0)	−2.7 (−11.9)				
6 + 13 → 19	−39.3	8.9 (2.4)	16.9 (10.3)	16.4 (9.8)	−32.1	12.1 (11.5)	18.6 (18.0)	18.4 (17.8)
19 → 20	−2.2	−15.0 (−16.4)	−14.6 (−16.0)	−14.9 (−16.3)	0.4	2.4 (3.7)	2.3 (3.7)	2.0 (3.4)
20 → 21	8.0	−1.0 (2.6)	−2.6 (1.0)	−1.9 (1.7)	2.3	3.4 (6.2)	2.9 (5.7)	3.3 (6.1)
21 → 17A	−9.5	−5.5 (−10.2)	−3.6 (−8.3)	−2.3 (−7.0)	−8.4	0.3 (−0.5 <sup>c</sup> )	2.0 (1.2)	2.5 (1.7)
19	−43.8	−16.6 (−25.0)	−7.7 (−16.1)	0.2 (−8.2)				
17A + 2 → 23	−36.6	−4.6 (−11.9)	2.8 (−4.4)	10.0 (2.8)				
23 → 22	−7.3	−11.9 (−13.2)	−10.5 (−11.7)	−9.8 (−11.0)	−2.1	−0.3 <sup>b</sup> (4.2)	0.1 (4.7)	−0.4 <sup>b</sup> (4.2)
20	8.6	−5.7 (−4.1)	−7.5 (−5.8)	−8.2 (−6.5)				
22 → 24	4.2	3.5 (3.3)	2.6 (2.5)	1.0 (0.9)	−6.8	9.0 (5.3)	10.4 (6.6)	9.3 (5.5)
24 → 25A	4.4	−9.2 (−7.4)	−10.1 (−8.3)	−9.2 (−7.4)	3.1	8.5 (14.4)	7.8 (13.8)	7.7 (13.7)
21	42.2	10.2 (22.8)	1.6 (14.2)	0.0 (12.6)				
22	−46.7	−9.8 (−18.1)	−0.3 (−8.6)	0.7 (−7.6)				
8A + 13 → 26	−34.4	17.4 (13.6)	24.4 (20.6)	23.6 (19.8)				
26 → 27	−4.3	−15.9 (−17.4)	−15.0 (−16.5)	−15.1 (−16.6)	0.3	1.7 (3.2)	1.6 (3.1)	1.5 (3.0)
27 → 28	7.7	−0.6 (3.7)	−2.1 (2.1)	−1.3 (2.9)	3.6	3.5 (6.2)	2.8 (5.5)	3.4 (6.1)
28 → 22	−15.7	−10.7 (−18.1)	−7.5 (−14.9)	−6.4 (−13.8)	−7.8	−0.6 <sup>b</sup> (−2.0 <sup>c</sup> )	1.0 (−0.5 <sup>c</sup> )	1.6 (0.1)
23	−36.4	−9.8 (−19.1)	−2.4 (−11.7)	−1.4 (−10.7)				
11A → 32	6.6	22.0 (25.7)	20.7 (24.4)	19.6 (23.3)	−2.4	21.6 <sup>b</sup> (25.4 <sup>c</sup> )	22.1 (25.9)	(24.9 <sup>c</sup> )
32 + 13 → 33	−47.1	−2.9 (−12.9)	6.7 (−3.3)	6.8 (−3.2)				
33 → 34	−1.5	−16.7 (−19.0)	−16.3 (−18.7)	−16.3 (−18.7)	−1.8	1.4 (1.9)	1.8 (2.3)	1.8 (2.3)
34 → 35	6.7	−0.5 (4.5)	−1.8 (3.2)	−1.2 (3.8)	3.9	3.7 (6.8)	2.9 (6.0)	3.4 (6.5)
35 → 29	−1.0	−11.8 (−17.4)	−11.6 (−17.2)	−10.4 (−16.0)	−3.4	−0.8 <sup>b</sup> (−1.2 <sup>c</sup> )	−11.6 <sup>b</sup> (−0.6 <sup>c</sup> )	−11.0 <sup>b</sup> (0.0)

Table 1. Continued

reacn	$\Delta S^\circ$	$\Delta H^\circ$	$\Delta G^\circ$	$\Delta G^\circ_{\text{solv}}$	$\Delta S^\ddagger$	$\Delta H^\ddagger$	$\Delta G^\ddagger$	$\Delta G^\ddagger_{\text{solv}}$
24	−6.4	−9.6 (−9.6)	−8.3 (−8.3)	−8.9 (−8.9)				
29 → 36	−4.7	8.2 (7.5)	9.2 (8.5)	7.9 (7.2)	−17.7	15.7 (11.9)	19.3 (15.5)	18.1 (14.3)
36 → 30	−1.7	−17.8 (−17.1)	−17.5 (−16.8)	−16.7 (−16.0)	−0.7	9.5 (14.7)	9.6 (14.8)	8.9 (14.1)
25	47.2	11.4 (24.2)	1.8 (14.6)	0.1 (12.9)				
26	−40.4	−16.7 (−23.5)	−8.5 (−15.3)	−0.5 (−7.3)				
31 + 2 → 37	−44.6	−2.5 (−11.8)	6.6 (−2.8)	14.4 (5.0)				
37 → 11A	4.1	−14.2 (−11.7)	−15.0 (−12.6)	−14.6 (−12.2)	7.1	3.5 (7.3)	2.0 (5.9)	2.2 (6.1)

<sup>a</sup> Calculation at the RI-MP2/Λ1//PBE/3ζ level. <sup>b</sup> Accounting for thermal corrections leads to the disappearance of the activation barriers. <sup>c</sup> Accounting for energy corrections (MP2) leads to the disappearance of the activation barriers.

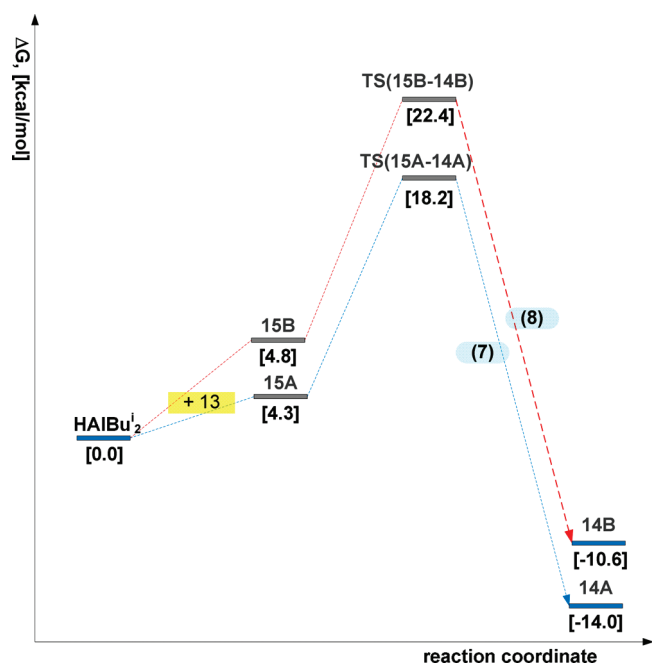


Figure 1. Energetic profile of reactions 7 and 8 (Gibbs reaction energies in kcal/mol are shown in brackets).

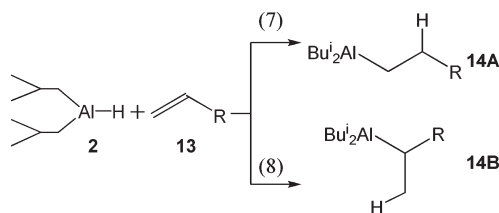
dimeric, and trimeric forms of  $\text{HAIBu}_2$ , leading to the formation of  $\text{Cp}_2\text{ZrHCl}$ , were also studied.<sup>18b</sup> It was shown that the reactions including an associated form of  $\text{HAIBu}_2$  are hampered by high activation barriers. Therefore, the catalytic hydroalumination reaction with  $\text{HAIBu}_2$ , monomeric form, being forestalled by dissociative processes is quite probable. The modeling of the  $\text{Cp}_2\text{ZrCl}_2$  reaction with  $\text{HAIBu}_2$  dimer and trimer will be reported elsewhere.

First, we studied the noncatalytic reaction of a terminal alkene (propene) with monomeric  $\text{HAIBu}_2$ . Propene was chosen to reduce calculation time and to study the regioselectivity of the reaction. Second, the interaction of the propene with Zr,Al-hydride complexes was examined with the consideration of the transmetalation stages. The complexes that have an available M–H bond in their structure and may directly react with alkenes were considered as potentially active centers of the catalytic hydroalumination. This is why we studied the mono- and bimetallic complexes  $\text{Cp}_2\text{ZrHCl}$  (5),  $[\text{Cp}_2\text{ZrH}_2 \cdot \text{ClAlBu}_2]$  (6),  $[\text{Cp}_2\text{ZrH}_2 \cdot \text{HAIBu}_2 \cdot \text{ClAlBu}_2]$  (8A), and  $[\text{Cp}_2\text{ZrH}_2 \cdot (\text{HAIBu}_2)_2]$  (11A) (Scheme 1) as hypothetically active species of the reaction. The high probability of complex formation in the studied system was shown in our previous work.<sup>1</sup> Furthermore, dimeric

complex 7, which was observed experimentally,<sup>6</sup> should not exhibit any hydrometalation activity because it does not contain a free Zr–H bond. However, complex 7 readily reacted with alkenes.<sup>6</sup> Probably, in this case the olefin interacts with monomer 6, which is in dynamic equilibrium with complex 7.

In this work, we did not take into account the participation of  $\text{ClAlBu}_2$  (which is the product of  $\text{HAIBu}_2$  transformation) in the catalytic process. These assumptions are sufficiently substantiated because under catalytic conditions the concentration of  $\text{ClAlBu}_2$ , which forms at the initial stages of the process, is considerably lower than that of  $\text{HAIBu}_2$ ; therefore, the contribution of  $\text{ClAlBu}_2$  can be disregarded.

**Propene Hydroalumination by  $\text{HAIBu}_2$ .** Noncatalytic propene hydroalumination by  $\text{HAIBu}_2$  can occur in two ways: (i) attachment of a terminal C atom of the propene double bond to Al, providing the anti-Markovnikov product *n*-propyldiisobutylaluminum (14A; reaction 7), and (ii) coordination of an internal C atom to the metal center, producing the Markovnikov product isopropyldiisobutylaluminum (14B; reaction 8) (Figure S1).



Thermodynamic parameters of these reactions are shown in Table 1. Figure 1 demonstrates higher probability of reaction 7 in comparison with pathway 8.

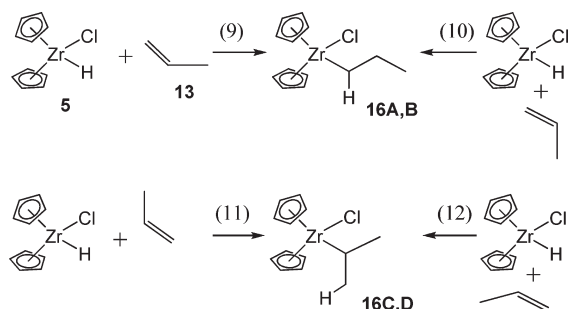
It was found<sup>19</sup> that noncatalytic alkene hydroalumination occurs via formation of a  $\pi$  complex. For example, the calculation of the electron energy change in the reaction of  $\text{AlH}_3$  with ethylene at the MP4/6-311+G(d,p)//HF/3-21G(d) level of theory<sup>19a</sup> shows exothermic formation of the prereaction  $\pi$  complex ( $\Delta E = -9.6$  kcal/mol). We found  $\pi$  complexes 15A, B and transition states TS(14A-15A) and TS(14B-15B) in reactions 7 and 8 (Figure S1 and Figure 1) by scanning the potential energy surface (PES) of the noncatalytic system. Further calculations showed that the activation barrier ( $\Delta G^\ddagger$ ) is 3.7 kcal/mol lower for the anti-Markovnikov product (14A) than for the Markovnikov product (14B). In transition state TS(14A-15A) the bond lengths Al–H and Al–C are 1.768 and 2.149 Å, respectively. Approximately, the same interatomic distances were estimated<sup>19b</sup> for the transition state of the  $\text{AlH}_3$  reaction with ethylene ( $r_{\text{Al-H}} = 1.668$  Å and  $r_{\text{Al-C}} = 2.154$  Å calculated by MP2/6-311+G(d)) and propene ( $r_{\text{Al-H}} = 1.666$  Å



and  $r_{\text{Al}-\text{C}} = 2.090 \text{ \AA}$  calculated by HF/6-311+G(d)). The activation barrier comparison for reactions 7 and 8 in Figure 1 counts toward the higher probability of **14A** formation.

Thus, the noncatalytic interaction of monomeric  $\text{HAlBu}_2^i$  with propene is possible and could occur in reactive media without a catalyst if the monomer concentration is sufficiently high. Probably, in the case of thermal hydroalumination, the elevated temperatures help to increase the effective concentration of  $\text{HAlBu}_2^i$  monomer.

**Catalytic Cycle with  $\text{Cp}_2\text{ZrHCl}$ .** 1. *Reaction of  $\text{Cp}_2\text{ZrHCl}$  with Propene.* Previous theoretical investigation on the  $\text{Cp}_2\text{ZrHCl}$  interaction with ethylene<sup>8</sup> provided two paths of the alkene coordination to the Zr–H bond. In the reaction with propene, a nonequivalency of multiple bond carbon atoms provides two additional possibilities for the substrate coordination. Therefore, we studied the attachment processes for (i) propene terminal, (ii) internal double bond carbon atoms to Zr between H and Cl atoms (reactions 9 and 11), and from the outside of Zr–H bond (reactions 10 and 12). As a result, reactions 9 and 10 provide conformers of zirconocene *n*-propyl chloride (**16A,B**), whereas reactions 11 and 12 give conformers of zirconocene isopropyl chloride (**16C,D**), respectively (Figure 2). Figure 3 shows energy profiles for reactions 3–6 (Scheme 1).



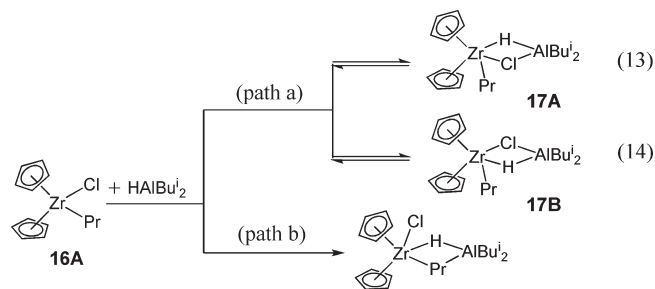
The following transition states preceding **16A–D** complexes have been found: **TS(5-16A)** and **TS(5-16B)** for reactions 9 and 10 and **TS(5-16C)** and **TS(5-16D)** for reactions 11 and 12 (Figure 2, 3).

Among the four complexes **16A–D**, Gibbs formation energies for *n*-propyl-substituted complexes **16A,B** are the lowest (Table 1). However, reaction 9, providing **16A**, is characterized by the lowest energy barrier ( $\Delta G^\ddagger = 10.4 \text{ kcal/mol}$ ). Moreover, alkene coordination to the Zr–H bond from the cyclopentadienyl ligand side (reactions 10 and 12) goes over comparatively high activation barriers (23.4 and 26.8 kcal/mol); this can be explained by steric difficulties. Thus, the alkene insertion proceeds mainly from the inner H–Zr–Cl corner of the molecule  $\text{Cp}_2\text{ZrHCl}$ ; this is in good agreement with calculations for similar reactions with ethylene.<sup>8</sup>

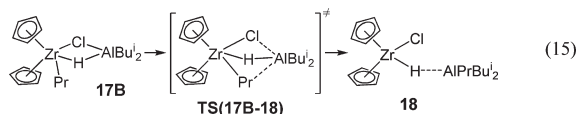
Because of the activation energies for reactions 9 and 11 being close, it can be assumed that Zr complexes containing the isopropyl fragment are formed along with *n*-propyl-substituted complexes at the beginning of the reaction. However, with time  $\text{Cp}_2\text{ZrPr}^n\text{Cl}$  eventually isomerizes into a complex with an alkyl of normal structure.<sup>5,20</sup> Consequently, the product of the examined hydrozirconation reaction is  $\text{Cp}_2\text{ZrPr}^n\text{Cl}$ .<sup>21</sup>

II. *Transmetalation Reaction of  $\text{Cp}_2\text{ZrPr}^n\text{Cl}$  with  $\text{HAlBu}_2^i$ .* Taking into account the tendency of  $\text{HAlBu}_2^i$  association with

zirconium complexes via bridge bonds, it can be supposed a priori that transmetalation reaction runs via formation of either chlorine-hydrogen (path a) or alkyl-hydrogen (path b) bridges:



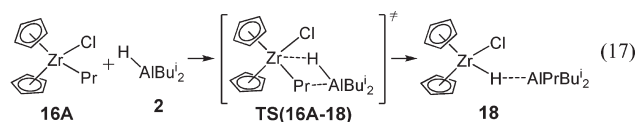
In fact, interaction of  $\text{Cp}_2\text{ZrPr}^n\text{Cl}$  (**16A**) with  $\text{HAlBu}_2^i$  via the pathway (a) goes through reactions 13 and 14 and gives the two isomeric complexes **17A,B** (Figure 2). Complex **17A** is formed as a result of  $\text{HAlBu}_2^i$  molecule orientation along the Zr–H bond from the outer side of the Cl–Zr–C angle and in **17B** from the inner side. Thermodynamically, formation of **17A** is 3.4 kcal/mol more favorable than that of **17B**. Reactions 13 and 14 are reversible ( $\Delta G^\circ_7 = -14.3 \text{ kcal/mol}$ ,  $\Delta G^\circ_8 = -10.9 \text{ kcal/mol}$ ); therefore, the isomerization **17A**  $\leftrightarrow$  **17B** can run through complex **16A**. The existence of such an interconversion is important, because we found that, unlike that of **17A**, the structure of complex **17B** is suitable for further intermolecular transformation, which provides associate **18** (reaction 15, Figure 2). In fact, complex **18** is a hydroalumination product, in which alkylalane is coordinated with  $\text{Cp}_2\text{ZrHCl}$  via a Zr–H–Al bridge bond. On the PES of reaction 15, transition state **TS(17B-18)** is found, and its activation energy is 23.0 kcal/mol (Figure 3). In the framework of the applied quantum chemical approximation of the transition state, a similar reaction for **17A** is not observed.



The decomposition of associate **18** (reaction 16) gives alkylalane (**14A**) and regenerates  $\text{Cp}_2\text{ZrHCl}$  (**5**):



Despite the fact that the formation of chlorine–hydrogen bridge bonds is thermodynamically more favorable (path a), we found an alternative mechanism for the single-stage transmetalation of **16A** by the  $\text{HAlBu}_2^i$  molecule into **18** (path b, reaction 17). The structure with alkyl–hydrogen bridges **TS(16A-18)** corresponds to the activation barrier peak (Figure 2).



The  $\Delta E^\ddagger$  values of reaction 17 calculated by the RI-MP2/ $\Delta 2//\text{PBE}/3\zeta$  approach were found to be negative. Apparently, the transition state **TS(16A-18)** is an artifact of the DFT

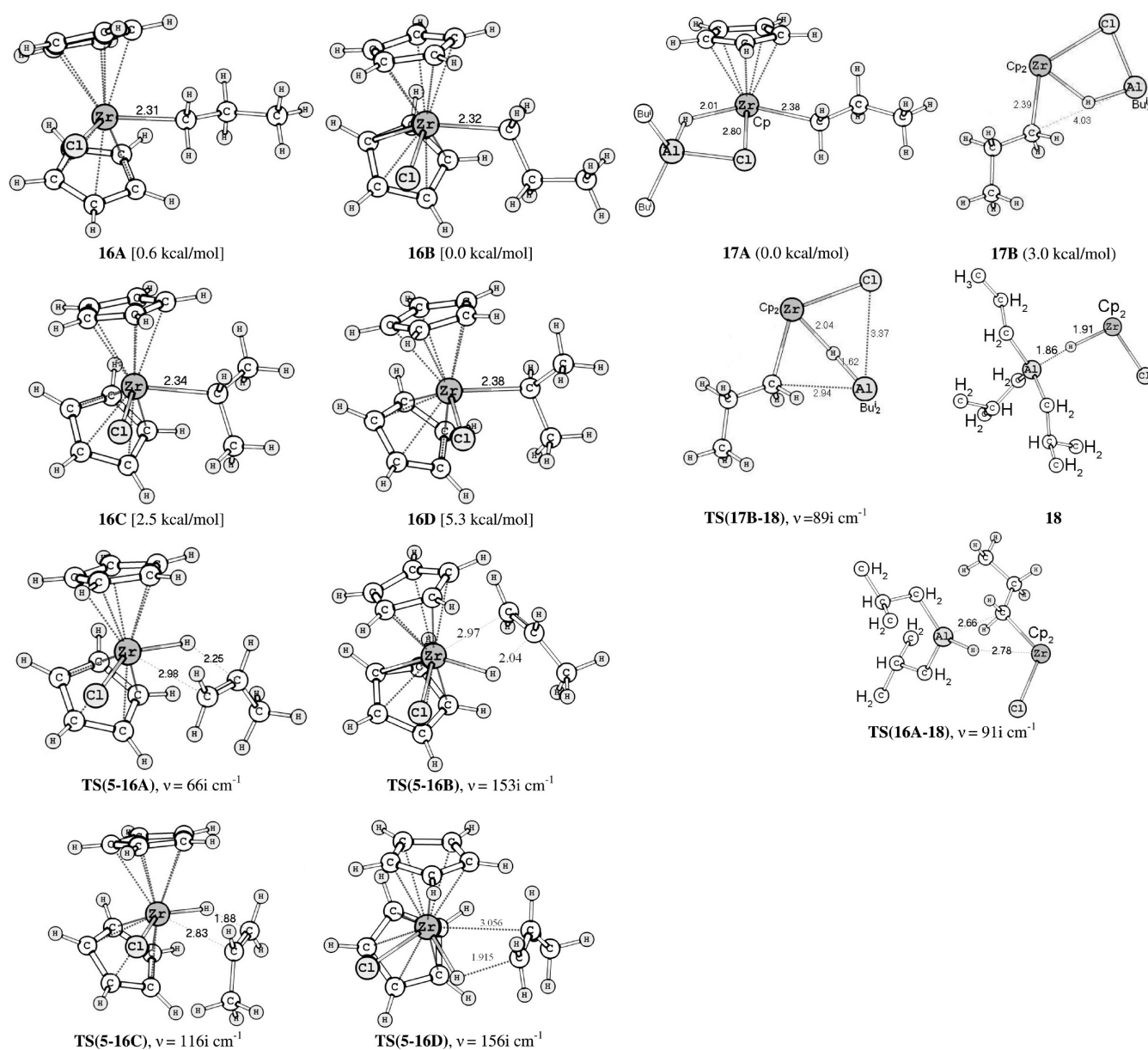


**Figure 2.** Structures of the complexes which correspond to the state points on the PES of propene reaction with  $\text{Cp}_2\text{ZrHCl}$  (5) and transmetalation stages 15–17.

method, which does not always reproduce well the transformation energy including bridge bonds. The reaction occurs via formation of the  $\text{Zr}-\text{Pr}-\text{Al}$  and  $\text{Zr}-\text{H}-\text{Al}$  bridge bonds (there is a vacant coordination site on the zirconium atom in complex 16A). As was mentioned above, the PBE/3 $\zeta$  approximation is characterized with different quality in descriptions of weak  $\text{Zr}-\text{Pr}-\text{Al}$  and relatively strong  $\text{Zr}-\text{H}-\text{Al}$  bridge bonds. Since synchronous cleavage of the  $\text{Zr}-\text{C}$  bond and formation of the  $\text{Zr}-\text{H}$  bond compensate the energy costs of the restructuring of the molecular system, the observed problem of negative activation energy may be caused by the inadequacy of the description of this compensation.

Thus, the catalytic cycle with  $\text{Cp}_2\text{ZrHCl}$  (5) participation can be represented by Scheme 2.

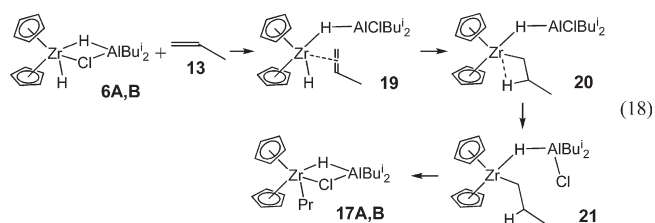
Catalytic cycle A includes four stages: alkene hydrozirconation (reaction 9), addition of the OAC molecule to zirconocene

alkylchloride (reaction 14), and transmetalation (reaction 15) followed by the decomposition of complex 18 on alkylalane 14A and the initial catalytic center 5 (reaction 16). The stage of hydrozirconation (reaction 9) has the highest activation barrier. The barrier of reaction 17 and preliminary estimation of kinetic constants<sup>26</sup> suggest that direct single-stage transmetalation prevails.

The possibility of a second OAC molecule interaction with complex 17A (17B) is examined further below.

**Catalytic Cycle with  $[\text{Cp}_2\text{ZrH}_2 \cdot \text{CpAlBu}_2]$  (6A,B) and  $[\text{Cp}_2\text{ZrH}_2 \cdot \text{HAlBu}_2 \cdot \text{CpAlBu}_2]$  (8A) Complexes.** The presence of a considerable quantity of  $\text{HAlBu}_2$  in the reaction media makes it possible to form a number of complicated bimetallic  $\text{Zr}, \text{Al}$  complexes.<sup>1</sup> Therefore, we have investigated the possibility of alkene reaction with bimetallic hydride  $\text{Zr}, \text{Al}$  complexes as catalytically active centers in alkene hydroalumination.

**I. Propene Hydrozirconation by Complexes 6A,B.** We have previously shown that the reaction of  $\text{Cp}_2\text{ZrHCl}$  with  $\text{HAlBu}_2^i$  provides the isomeric complexes **6A,B**, which have similar energies and differ only in the position of bridge bonds  $\text{Zr}-\text{H}-\text{Al}$  and  $\text{Zr}-\text{Cl}-\text{Al}$ . Propene addition to complexes **6A,B** (reaction 18) gives bridge complexes with alkyl substitution **17A,B** (Figure 4).



Reaction 18 includes several elementary stages. At the first stage we observed breaking of the  $\text{Zr}-\text{Cl}$  bond, which is the weakest among the two bridge bonds in complexes **6A,B** ( $\Delta G^\ddagger = 17.8$  kcal/mol) (Table 1). This makes it easier for alkene to approach the zirconium atom. On the PES of reaction 18 (Figure 5), the local minimum **19** and transition state **TS(6-19)** were located. The  $\text{Zr}-\text{Cl}$  distance increases from 2.76 Å in compound **6** to 4.24 Å in **TS(6-19)**. The structure of **19** is close to that of **6**; however, complex **19** has an “open” geometry with a free  $\text{Zr}-\text{H}$  bond. Therefore, the breaking of the  $\text{Zr}-\text{Cl}$  bond eliminates the structural difference between isomers **6A,B** and further transformations occur with the “open” complex **19**.

The next stage is the reaction of the alkene hydrozirconation with complex **19**. The transition state **TS(19-20)** and local minimum **20** were found on the PES of this process.

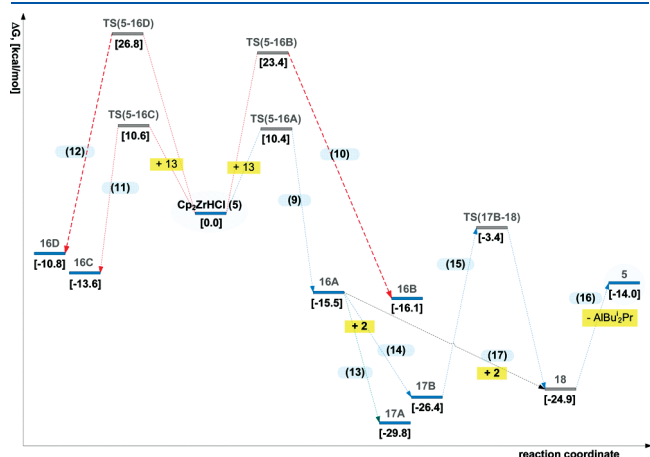
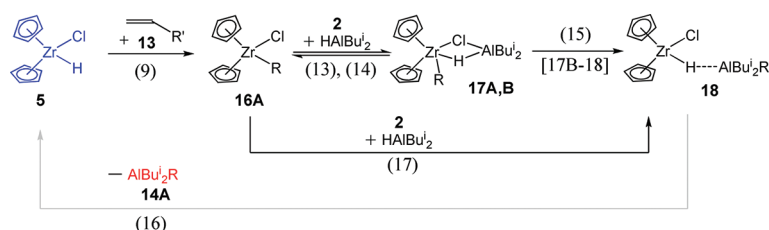


**Figure 3.** Energetic profile of propene reaction with  $\text{Cp}_2\text{ZrHCl}$  (**5**) and transmetalation stages **15–17**.

## Scheme 2. Catalytic Cycle A

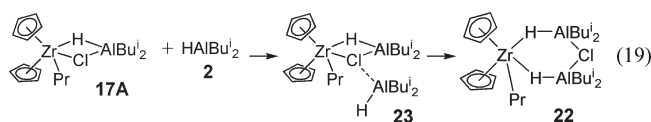


The activation barrier of the reaction is only 3.4 kcal/mol, which is 3-fold less than that for the reaction of propene hydrozirconation by  $\text{Cp}_2\text{ZrHCl}$  (reaction 9,  $\Delta G^\ddagger = 10.4$  kcal/mol). Moreover, the structure and geometric parameters of the new **TS(19-20)** (Figure 4) differ from the corresponding characteristics of the direct hydrozirconation TS examined above. If in **TS(5-16A)** and **TS(2-14A)**  $\text{M}-\text{H}\cdots\text{C}-\text{C}$  bonds lie on one flat surface, then the planarity in **TS(19-20)** is distorted, obviously, due to steric interaction with the neighboring organoaluminum fragment. The  $\text{H}-\text{C}$  bond length increases by 0.3 Å in **TS(19-20)** compared to that in **TS(5-16A)** (from 2.25 Å to 2.55 Å).

As a result, the alkene hydrozirconation by complex **19** gives products **20** and **21**. The agostic interaction  $\text{Zr}-\text{H}_{\text{alkyl},\beta}$  was observed in complex **20**: the  $\text{Zr}-\text{H}_{\text{alkyl},\beta}$  distance is 2.12 Å, and  $\angle\text{Zr}-\text{C}-\text{C} = 84.9^\circ$ . The transformation **20**  $\rightarrow$  **21** running through transition state **TS(20-21)**, where the  $\text{Zr}-\text{H}_{\text{alkyl},\beta}$  dative bond should be broken, is thermodynamically probable ( $\Delta G^\circ = 1.7$  kcal/mol,  $\Delta G^\ddagger = 6.1$  kcal/mol).

Summarizing the number of stages of alkene hydrozirconation by complex **19**, it should be noted that organoaluminum fragment of the complex does not participate in the reaction: i.e., the distance between chlorine and zirconium atoms in the intermediates is constantly great (Figure 4). At the end of the reaction, the  $\text{Zr}-\text{Cl}-\text{Al}$  bridge bond in complex **17A** is formed almost with no barrier. Locking of **21** into a four-membered cycle could give **17B** as well.

**II. Transmetalation of Complex 17A with  $\text{HAlBu}_2^i$ .** In excess OAC, complexes **17A,B** can interact with the  $\text{HAlBu}_2^i$  molecule. The transmetalation of complexes **17A,B** by  $\text{HAlBu}_2^i$  has been studied in the example of **17A**. Energetic characteristics of reaction 19 are presented in Table 1 and in Figure 5.

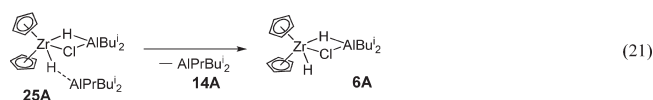
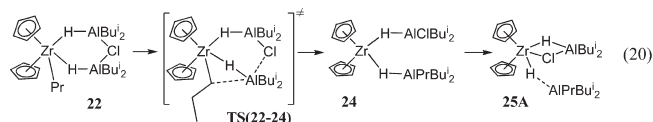


The formation of a six-membered  $\text{Zr},\text{Al}$  complex of cyclic structure **22** (Figure 4) from **17A** occurs through local minimum **23** and **TS(22-23)**. Structure **22** is similar to **8A**, in which the hydrogen atom is substituted with an alkyl group.

The intramolecular process of propyl group transfer from the zirconium to the aluminum atom (transmetalation reaction 20) runs through two stages: **22**  $\rightarrow$  [**TS(22-24)**]  $\rightarrow$  **24**  $\rightarrow$  [**TS(24-25)**]  $\rightarrow$  **25A**. The energy barriers  $\Delta G^\ddagger$  of reaction 20 are 5.5 kcal/mol (**22**  $\rightarrow$  **24**) and 13.7 kcal/mol (**24**  $\rightarrow$  **25A**); these barriers are less than that of reaction 15 ( $\Delta G^\ddagger = 23.0$  kcal/mol, Figure 4, Table 1). Similarly to complex **21**, formation of the  $\text{Zr}-\text{Cl}-\text{Al}$  bridge in **24** could provide isomeric compounds **25A**,

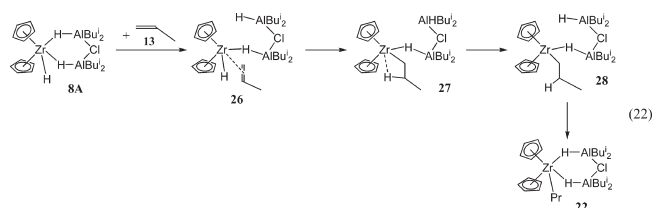


B. As a result, for example, complex **25A** can be formed in reaction 20, and its subsequent dissociation in reaction 21 gives alkylalane **14A** and the Zr,Al complex **6A**. We could not locate a transition state for the latter transformation at the level of theory used in this work.



III. Propene Hydrozirconation by Complex **8A**. A high tendency of OACs to form associates suggests a possibility of different Zr,Al complex formation in 1:2 proportions; for example, trihydride clusters **8A** and **11A**.<sup>1,7</sup> Their reactivity in the reactions with alkenes also deserves special attention.

Complex **8A** is formed in reaction of complexes **6A,B** with  $\text{HAlBu}_2^i$ ; this process has an activation barrier of 8.4 kcal/mol.<sup>1</sup> The interaction of the alkene with **8A** (reaction 22) gives dihydride complex **22**. Since further transformations of **22** are presented in section II, here we analyze reaction 22 in detail.



In complex **8A** the zirconium atom is pentacoordinated; consequently, alkene insertion into the Zr–H bond occurs after one of the coordination sites at the metal atom becomes free (similar to the case for complexes **6A,B**). Complex **8A** contains two energetically close Zr–H bridge bonds, dissociation of which requires 19.8 kcal/mol (see diagram in Figure 5). This value is considerably higher than the dissociation barrier of the Zr–Cl bond in complexes **6A,B**. This fact confirms the hypothesis that complex **8A** should be less active among the other catalytic centers in the hydrometalation reaction. On the PES of reaction 22 extrema **26**, **TS(26-27)**, **27**, **TS(27-28)**, **28**, and **TS(28-22)** were located (Figure S4).

Further, we focused our attention on **TS(26-27)** because its structure is close to that of **TS(19-20)** (C–H<sub>alkyl</sub> and Zr–C distances are the same within 0.01 Å). The energy barrier of the alkene hydrozirconation with complex **26** is 0.4 kcal/mol lower than that in the reaction with complex **19**. The interacting bonds in **TS(26-27)** are not coplanar, similar to the case for **TS(19-20)**.

Scheme 3 represents catalytic cycle B, which includes stages of propene hydroalumination by complexes **6A,B** and **8A**: interaction of propene with complexes **6A,B** (stage 18) and **8A** (stage 22), addition of the  $\text{HAlBu}_2^i$  molecule to **17A,B** (stage 19), transmetalation of intermediate **22** into **25A,B** (stage 20), and dissociation of **25A,B** to give alkylalane **14A** and complexes **6A,B** (stage 21). Thus, the alkene reaction with the bimetallic complexes is a multistage process, whereas the reaction with  $\text{Cp}_2\text{ZrHCl}$  runs via one step. The least energetically favorable and, therefore, the limiting stages of catalytic cycle B are the stages of Zr–Cl and Zr–H bridge

bond breaking in complexes **6A,B** and **8A**, respectively. The further transformations have insignificant activation barriers. It is interesting that the four-centered transition states **TS(19-20)** and **TS(26-27)** located on the PES of reactions 18 and 22 have nonplanar structures due to the steric effect of the bulky organoaluminum fragment. This feature could affect the stereoselectivity of the hindered alkene hydroalumination (see, for example, ref 6c).

**Catalytic Cycle with the Complex  $[\text{Cp}_2\text{ZrH}_2 \cdot (\text{HAlBu}_2^i)_2]$  (**11A**).** Complex **11A** is a result of barrier-free consecutive transformations of **8A** (Scheme 1).<sup>1</sup> Nevertheless, it should be considered as possible intermediate of the alkene hydroalumination reaction (Scheme 4).

The elementary stages of catalytic cycle C for **11A** are analogous to the corresponding stages of **8A**: alkene hydrozirconation (reaction 23), a transmetalation stage (reaction 24), alkylalane formation (reaction 25), and the initial intermediate regeneration (reaction 26).

The structures of all the complexes corresponding to the stationary points of reactions 23–26 are presented in Figure S5. Thus, on the PES of reaction 23 extrema **TS(11A-32)**, **32**, **33**, **TS(33-34)**, **34**, **TS(34-35)**, **35**, **TS(29-35)**, and **29** were located. Reaction 24 goes through **TS(29-36)**, local minimum **36**, and **TS(30-36)**. On the PES of reaction 26 the local minimum **37** and **TS(11A-37)** were found. The energy diagram of the complex transformations is presented in Figure 6.

In catalytic cycle C, there are two stages with high activation barriers: (a) alkene insertion (reaction 23,  $\Delta G^\ddagger = 23.3$  kcal/mol) and (b) transmetalation (reaction 24,  $\Delta G^\ddagger = 14.3$  kcal/mol). These barriers are much higher than the barriers of the corresponding stages 22 and 20 for complex **8A**. Moreover, Scheme 4 implies the participation of intermediate **31**, the reactivity of which should be less than that of complexes **6A,B**, because of the stronger bridge Zr–H bond in comparison with Zr–Cl (for example, the  $\Delta G^\ddagger$  value for Zr–H bridge bond dissociation in **11A** is 23.3 kcal/mol, whereas  $\Delta G^\ddagger$  for bridge Zr–Cl bond breaking in **6A,B** is equal to 17.8 kcal/mol). Indeed, according to experimental data,<sup>6c</sup> a compound with a structure close to **31** is less active than dimeric complex **7**, the active form of which is monomer **6**. Thus, catalytic cycle C exists in isolation from the system of active centers within the hydroalumination reaction. Therefore, because of the predictably low activity of complex **11A**, we will not consider the catalytic cycle C in the general scheme while discussing the mechanism of the catalytic alkene hydroalumination.

**Mechanism of Alkene Hydroalumination by  $\text{HAlBu}_2^i$ , Catalyzed with  $\text{Cp}_2\text{ZrCl}_2$ .** Above we showed that complexes  $\text{Cp}_2\text{ZrHCl}$  (**5**),  $[\text{Cp}_2\text{ZrH}_2 \cdot \text{ClAlBu}_2^i]$  (**6**), and  $[\text{Cp}_2\text{ZrH}_2 \cdot \text{HAlBu}_2^i \cdot \text{ClAlBu}_2^i]$  (**8A**) may be considered as active centers of the catalytic alkene hydroalumination. Catalytic cycles A and B with corresponding intermediate transformations are summarized in Scheme 5.

According to Scheme 5, the first stage of the reaction  $\text{Cp}_2\text{ZrCl}_2 + \text{HAlBu}_2^i$  provides  $\text{Cp}_2\text{ZrHCl}$  (**5**), which further, in excess OAC ( $[\text{Zr}]:\text{OAC} = 1:3$ ), gives complexes **6A,B** and **8A**. Reactions  $5 \rightarrow 6A,B \rightarrow 8A$  should be very fast, because the consecutive addition of two  $\text{HAlBu}_2^i$  molecules to **5** has no activation barrier and the stages have practically irreversible character.<sup>1</sup> Therefore, under catalytic conditions, complex **8A** is thought to prevail in the reaction media. However, earlier<sup>6a,b</sup> we considered this complex as inactive in the

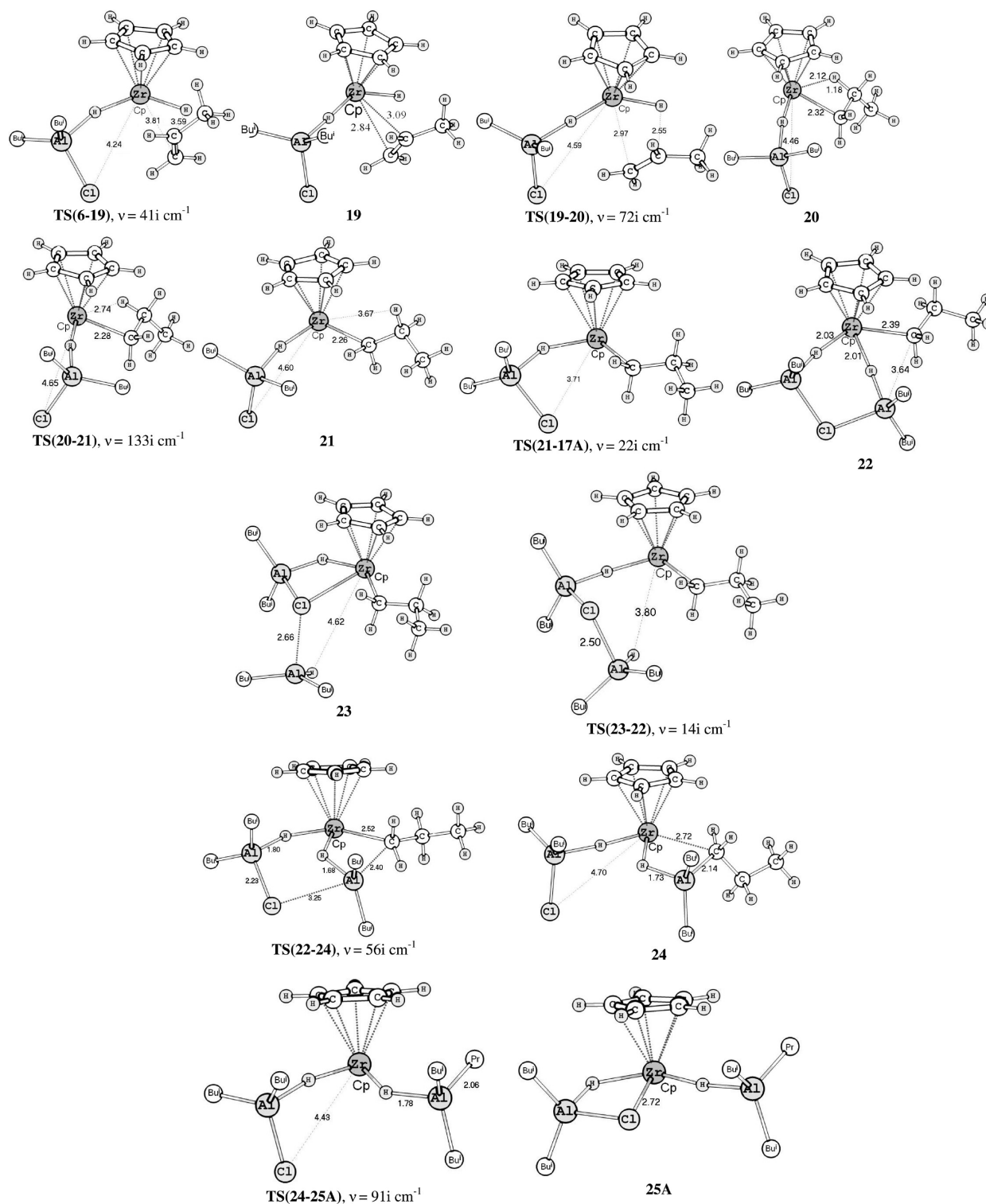


**Figure 4.** Structures of the complexes which correspond to the state points on the PES of reactions 18–20.

alkene hydroalumination, in contrast to the case for acetylenes,<sup>27</sup> because NMR monitoring showed the absence of the reaction products within 10 min after olefin addition to **8A** in a NMR tube. However, reinvestigation of the reaction<sup>28</sup> in a reactor with a magnetic stirrer exhibited 43% alkene conversion after 2 h (92% conversion within 20 h) and formation of a mixture consisting of **14A** and **16A**. The occurrence of **16A** proves

the consecutive involvement of complexes **6A,B** and **5** at the end of the alkene reaction with **8A**. Theoretical calculations showed that the reactivity of the hydride bimetallic complexes will be defined by the possibility of giving a free coordination place on Zr as a result of breaking Zr–H or Zr–Cl bridge bonds. Therefore, the highest barrier was observed in the case of the catalytic cycle beginning from

complex **8A** (reaction 22, 19.8 kcal/mol) over the activation barriers of the catalytic cycles starting from **6A,B** (reaction 18, 17.8 kcal/mol) and **5** (reaction 9, 10.4 kcal/mol). Thus, the activity of these complexes should increase in the series **8A** < **6A,B** < **5**. Consequently, the formed in situ  $\text{Cp}_2\text{ZrHCl}$  (**5**) is thought to be the most active center of the catalytic alkene hydroalumination. However, since this conclusion was based only on calculations of thermodynamics, it would be incorrect to make a choice between the intermediates in the case of a real catalytic system. Nevertheless, some predictions can be declared. First, under catalytic conditions the barrier-free sequential interactions should proceed as  $5 \rightarrow 6\text{A,B} \rightarrow 8\text{A}$ . The same result should be obtained in the reaction with a dimeric form of  $\text{HAlBu}_2$ : i.e.,  $5 + [\text{HAlBu}_2]_2 \rightarrow 8\text{A}$ . Therefore, the concentration of  $\text{Cp}_2\text{ZrHCl}$  formed in catalytic amounts at the first stages is negligible (or it does not “survive” at these conditions). Probably, for this reason  $\text{Cp}_2\text{ZrHCl}$  was not observed experimentally in the catalytic hydroalumination reactions.<sup>6a</sup> We can expect that  $\text{Cp}_2\text{ZrHCl}$  would significantly accelerate the reaction, but only in the case of an increased concentration of the catalyst (under stoichiometric conditions) or at the end of the catalytic reaction when the concentration of  $\text{HAlBu}_2$  will be reduced. From the other side, an increase of  $\text{HAlBu}_2$  concentration would raise the amount of complexes **8A** and **11A** having low activity and, therefore, would reduce the hydroalumination rate.

The degree of OAC self-association is an important factor as well. The computed Gibbs energy value for  $[\text{HAlBu}_2]_3$

dissociation ( $[\text{HAlBu}_2]_3 \leftrightarrow [\text{HAlBu}_2]_2 + \text{HAlBu}_2$ ) is sufficiently high:  $\Delta G^\circ_{203} = 12.6$  kcal/mol.<sup>18d</sup> Therefore, it should be expected that participation of the trimers  $[\text{HAlBu}_2]_3$  or dimers  $[\text{HAlBu}_2]_2$  will increase the activation barriers of steps  $5 \rightarrow 6\text{A,B} \rightarrow 8\text{A}$  and change the kinetic parameters of the hydroalumination reaction stages. However, this alternative does not exclude the existence of the proposed scheme, because the monomeric form  $[\text{HAlBu}_2]$  exists along with other associates at equilibrium concentration.<sup>18d,29</sup> Moreover, the monomer can be released through reversal stages 13, 14, and 19. Furthermore, Scheme 5 could be a part of the catalytic alkene reactions with  $\text{ClAlBu}_2$  or  $\text{AlBu}_3$ ; in these reactions  $\text{HAlBu}_2$  is formed at intermediate stages of the process as a result of  $\beta\text{-C-H}$  activation. Thus, further consideration of the dimeric and trimeric forms of  $\text{HAlBu}_2$  will expand the proposed scheme and a kinetic analysis of a generalized mechanism will determine an intermediate or intermediates, which would control the process flow depending on the reaction conditions.

#### Scheme 4. Catalytic Cycle C

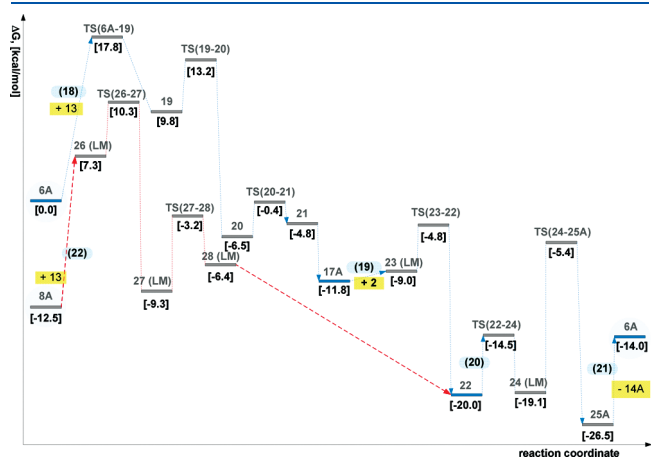
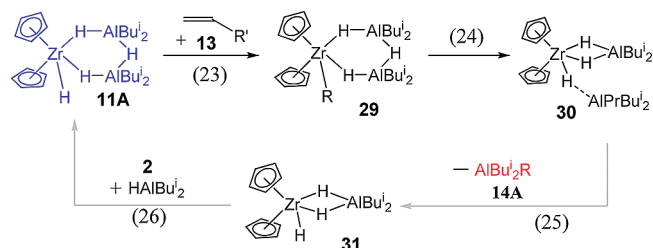


Figure 5. Energetic profile of propene reaction with complexes **6** and **8A**.

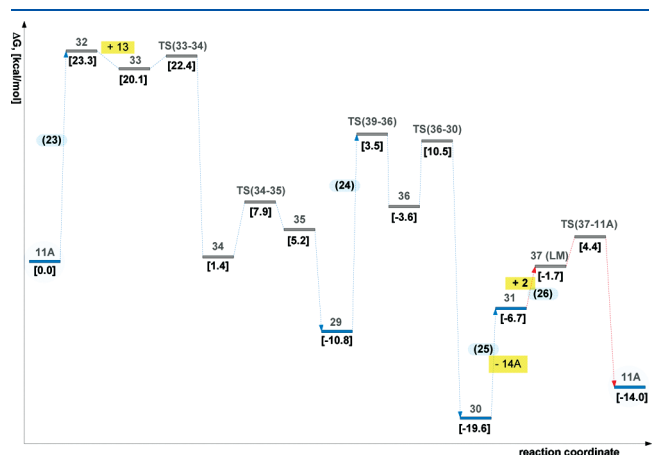
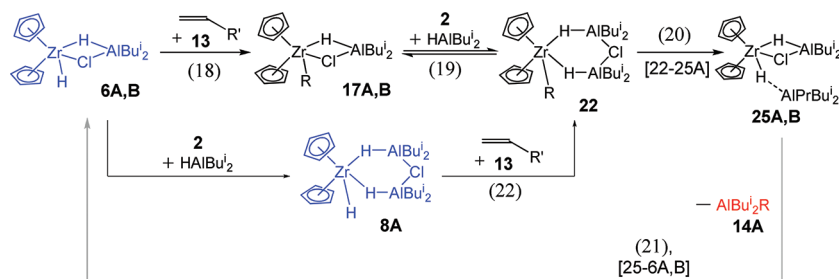
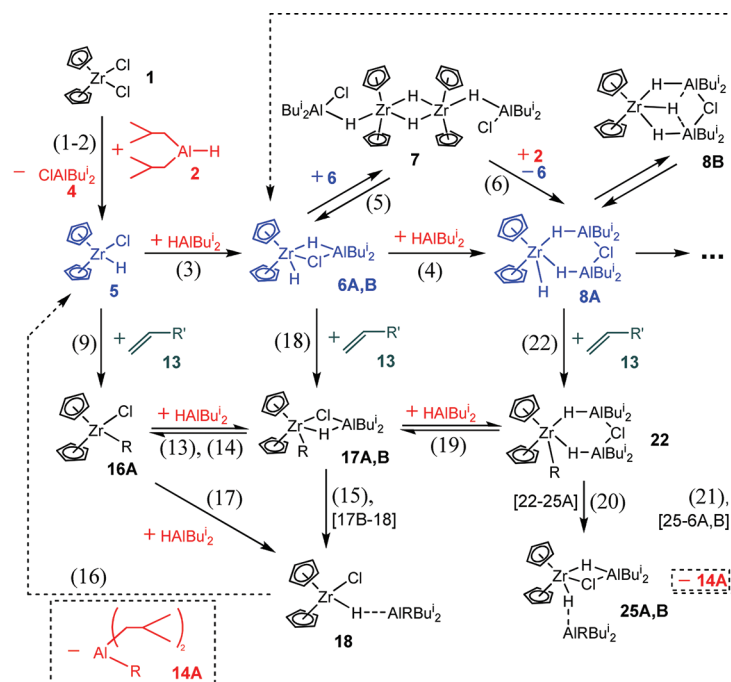


Figure 6. Energetic profile of the propene reaction with complex **11A**.

#### Scheme 3. Catalytic Cycle B



Scheme 5. Mechanism of Catalytic Alkene Hydroalumination by  $\text{HAlBu}_2^i$  with Active Centers 5, 6A,B, and 8A

## CONCLUSION

A detailed quantum chemistry study on the reaction of propene hydroalumination by  $\text{HAlBu}_2^i$  in the presence of  $\text{Cp}_2\text{ZrCl}_2$  has been carried out using PBE/3 $\zeta$  and RI-MP2/ $\Lambda 2$ /PBE/3 $\zeta$  approaches. It was shown that the PBE/3 $\zeta$  method correctly reproduces all the key regularities of the system studied at the MP2/ $\Lambda 2$  level (for example, the thermodynamics of Zr,Al-hydride complex formation and the relative hydrometalation activity of catalytic sites). Therefore, the PBE/3 $\zeta$  method can be used for a qualitative description of these metal complex systems.

Thus, the mechanism of catalytic alkene hydroalumination has been proposed (Scheme 5). The role of  $\text{Cp}_2\text{ZrCl}_2$  catalyst in alkene hydroalumination by  $\text{HAlBu}_2^i$  consists of the formation of active complexes  $\text{Cp}_2\text{ZrHCl}$  (5),  $[\text{Cp}_2\text{ZrH}_2 \cdot \text{ClAlBu}_2^i]$  (6A,B),  $[\text{Cp}_2\text{ZrH}_2 \cdot \text{HAlBu}_2^i \cdot \text{ClAlBu}_2^i]$  (8A), and  $[\text{Cp}_2\text{ZrH}_2 \cdot (\text{HAlBu}_2^i)_2]$  (11A), whose activity decreases in the series  $5 > 6A,B > 8A > 11A$ ; this is caused by the by an increase in the number of Zr–H–Al bridge bonds as a result of the consecutive  $\text{HAlBu}_2^i$  addition.

## ASSOCIATED CONTENT

**S Supporting Information.** This material is available free of charge via the Internet at <http://pubs.acs.org>.

## ACKNOWLEDGMENT

We thank the Foundation of the President of Russian Federation (Program for Support of Leading Scientific Schools, U.M.D., Grant NSh-2349.2008.3), the Russian Foundation of Basic Research (Grant No. 11-03-00210-a), and Zamaraev International Charitable Scientific Fund (E.Yu.P.) for financial support.

## REFERENCES

- (1) Pankratyev, E. Yu.; Tyumkina, T. V.; Parfenova, L. V.; Khalilov, L. M.; Khursan, S. L.; Dzhemilev, U. M. *Organometallics* **2009**, *28*, 968.
- (2) (a) Tolstikov, G. A.; Yuryev, V. P., *Aluminiyorganicheskiy sintez (Organoaluminium syntheses)*; Nauka: Moscow, 1979 (in Russian). (b) Tolstikov, G. A.; Dzhemilev, U. M.; Tolstikov, A. G., *Aluminiyorganicheskie soedineniya v organicheskom sinteze (Organoaluminium compounds in organic synthesis)*; Akad. izd. GEO: Novosibirsk, 2009 (in Russian). (c) Dzhemilev, U. M.; Ibragimov, A. G. Hydrometalation of unsaturated compounds. In *Modern Reduction Methods*; Andresson, P. G., Munslo, J. J., Eds.; Wiley-VCH: Weinheim, Germany, 2008.
- (3) Sato, F.; Sato, S.; Sato, M. *J. Organomet. Chem.* **1976**, *122*, C25.
- (4) Negishi, E.; Yoshida, T. *Tetrahedron Lett.* **1980**, *21*, 1501.
- (5) Hart, D. W.; Schwartz, J. *J. Am. Chem. Soc.* **1974**, *96*, 8115.
- (6) (a) Parfenova, L. V.; Pechatkina, S. V.; Khalilov, L. M.; Dzhemilev, U. M. *Russ. Chem. Bull., Int. Ed.* **2005**, *54*, 316. (b) Parfenova, L. V.; Balaev, A. V.; Gubaidullin, I. M.; Pechatkina, S. V.; Abzalilova, L. R.; Spivak, S. I.; Khalilov, L. M.; Dzhemilev, U. M. *Int. J. Chem. Kinet.* **2007**, *39*, 333. (c) Parfenova, L. V.; Vil'danova, R. F.; Pechatkina, S. V.; Khalilov, L. M.; Dzhemilev, U. M. *J. Organomet. Chem.* **2007**, *692*, 3424.
- (7) Baldwin, S. M.; Bercaw, J. E.; Brintzinger, H. H. *J. Am. Chem. Soc.* **2008**, *130*, 17423.
- (8) Endo, J.; Koga, N.; Morokuma, K. *Organometallics* **1993**, *12*, 2777.
- (9) (a) Laikov, D. N.; Ustynyuk, Y. A. *Russ. Chem. Bull., Int. Ed.* **2005**, *54*, 820. (b) Laikov, D. N. *Chem. Phys. Lett.* **1997**, *281*, 151. (c) Laikov, D. N. Ph.D. dissertation, Moscow State University, 2000 (in Russian).
- (10) Perdew, J. P.; Burke, K.; Ernzerhof, M. *Phys. Rev. Lett.* **1996**, *77*, 3865.
- (11) (a) Moller, C.; Plesset, M. S. *Phys. Rev.* **1934**, *46*, 618. (b) Frisch, M. J.; Head-Gordon, M.; Pople, J. A. *Chem. Phys. Lett.* **1990**, *166*, 275.
- (12) Laikov, D. N. *Chem. Phys. Lett.* **2005**, *416*, 116.
- (13) Neese, F. ORCA 2.6 Rev. 35: *An Ab Initio, DFT and Semiempirical electronic structure package*, 2008.
- (14) (a) Schafer, A.; Horn, H.; Ahlrichs, R. *J. Chem. Phys.* **1992**, *97*, 2571. (b) Eichkorn, K.; Treutler, O.; Ohm, H.; Haser, M.; Ahlrichs, R. *Chem. Phys. Lett.* **1995**, *240*, 283. (c) Eichkorn, K.; Weigend, F.; Treutler, O.; Ahlrichs, R. *Theor. Chem. Acc.* **1997**, *97*, 119.



- (15) Barone, V.; Cossi, M. *J. Phys. Chem. A* **1998**, *102*, 1995.
- (16) Besedin, D. V. *QCC Front-End 2.09*; 2005.
- (17) Zhurko, G. A.; Zhurko, D. A. *ChemCraft 1.6*; 2009.
- (18) (a) Pankratyev, E. Yu.; Tyumkina, T. V.; Khursan, S. L.; Parfenova, L. V.; Khalilov, L. M.; Dzhemilev, U. M. *Vestnik Bashkirskogo universiteta*, **2008**, *13*, 802 (in Russian). (b) Pankratyev, E. Yu. Ph.D. dissertation, Institute of Petrochemistry and Catalysis, Russian Academy of Sciences, 2010 (in Russian). (c) Pankratyev, E. Yu.; Tyumkina, T. V.; Khursan, S. L.; Khalilov, L. M. *Bashkirskiy Khimicheskiy Zhurnal*, **2010**, *17*, 28 (in Russian). (d) Pankratyev, E. Yu.; Khursan, S. L.; Tyumkina, T. V.; Khalilov, L. M. *J. Struct. Chem.* **2011**, *52*, 27.
- (19) (a) Bundens, J. W.; Francl, M. M. *Organometallics* **1993**, *12*, 1608. (b) Bundens, J. W.; Yudenfreund, J.; Francl, M. M. *Organometallics* **1999**, *18*, 3913.
- (20) Chirik, P. J.; Day, M. W.; Labinger, J. A.; Bercaw, J. E. *J. Am. Chem. Soc.* **1999**, *121*, 10308.
- (21) It is known that  $\beta$ -agostic interactions occur in the alkyl complexes of transition metals; this is manifested in the shortening of the distance between metal and hydrogen bonded with  $\beta$ -carbon atoms as well as in the unusually small angles  $M-C-C$ .<sup>22–25</sup> The configuration of the  $Cp_2ZrEtCl$  complex which demonstrates the agostic interaction was found by the MP2 method in ref 8. We performed relaxed geometry scans along the  $Zr-H_{alkyl}$  bond for both  $Cp_2ZrPr^iCl$  and  $Cp_2ZrEtCl$  complexes, using PBE/3 $\zeta$  and RI-MP2/ $\Delta$ 1 approximations. However, the agostic interactions in these complexes have not been found. Probably, the appearance of a local energy minimum point located by the authors<sup>8</sup> can be explained by the very small basis sets used (HW, 3-21G, STO-3G for different parts of the molecular system).
- (22) Brookhart, M.; Green, M. L. H. *J. Organomet. Chem.* **1983**, *250*, 395.
- (23) Weiss, H.; Haase, F.; Ahlrichs, R. *Chem. Phys. Lett.* **1992**, *194*, 492.
- (24) Jordan, R. F.; Bradley, P. K.; Baenziger, N. C.; LaPointe, R. E. *J. Am. Chem. Soc.* **1990**, *112*, 1289.
- (25) Bullock, R. M.; Lemke, F. R.; Szalda, D. J. *J. Am. Chem. Soc.* **1990**, *112*, 3244.
- (26) The reaction rate comparison of stages 15 and 17 at  $T = 203$  K is made assuming that irreversible decay of the **17B** intermediate along reaction 15 does not disturb the equilibrium of reaction 14: that is,  $W_{15} = k_{15}[17B] = k_{15}K_{14}[16A][2]$ . On the other hand,  $W_{17} = k_{17}[16A][2]$ , from which  $W_{15}/W_{17} = k_{15}K_{14}/k_{17} \approx 10^{-13}$ .
- (27) Carr, D. B.; Schwartz, J. *J. Am. Chem. Soc.* **1979**, *101*, 3521.
- (28) A flask equipped with a magnetic stirrer and filled with argon was loaded with 1.5 mmol of  $Cp_2ZrH_2$  and benzene (3 mL). Then, 1.5 mmol of  $HAlBu^i_2$  and 1.5 mmol of  $ClAlBu^i_2$  were added dropwise. The formation of complex **8A** was detected by NMR spectrometry. Hexene-1 (1.5 mmol) was added to the reaction mixture. The mixture was stirred for 20 h and analyzed by NMR. For the kinetic study, samples (0.2 mL) were syringed into tubes filled with argon, and the samples were decomposed with 10% HCl at 0 °C. The decomposition products were extracted with benzene; further, the organic layer was dried over  $Na_2SO_4$  and analyzed by GLC.
- (29) Vestin, R.; Vestin, U.; Kowalewski, J. *Acta Chem. Scand., Ser. A* **1985**, *39*, 767.